

# An inorganic–organic hybrid material based on a Keggin-type polyoxometalate@Dysprosium as an effective and green catalyst in the synthesis of 2-amino-4*H*-chromenes via multicomponent reactions

Sara Hosseinzadeh-Baghan<sup>1</sup> | Masoud Mirzaei<sup>1</sup>  | Hossein Eshtiagh-Hosseini<sup>1</sup> |  
Vahideh Zadsirjan<sup>2</sup> | Majid M. Heravi<sup>2</sup>  | Joel T. Mague<sup>3</sup>

<sup>1</sup>Department of Chemistry, Faculty of Science, Ferdowsi University of Mashhad, Mashhad, 917751436, Iran

<sup>2</sup>Department of Chemistry, School of Science, Alzahra University, PO Box 1993891176, Tehran, Vanak, Iran

<sup>3</sup>Department of Chemistry, Tulane University, New Orleans, LA, 70118, USA

## Correspondence

Masoud Mirzaei, Department of Chemistry, Faculty of Science, Ferdowsi University of Mashhad, 917751436 Mashhad, Iran.  
Email: mirzaesh@um.ac.ir

Majid M. Heravi, Department of Chemistry, School of Science, Alzahra University, PO Box 1993891176, Vanak, Tehran, Iran.  
Email: mmh1331@yahoo.com; mmheravi@alzahra.ac.ir

## Funding information

Ferdowsi University of Mashhad, Grant/Award Number: 3/42203

A novel inorganic–organic hybrid,  $[\text{Dy}_4(\text{PDA})_4(\text{H}_2\text{O})_{11}(\text{SiMo}_{12}\text{O}_{40})] \cdot 7\text{H}_2\text{O}$  denoted as (POM@Dy-PDA), based on a lanthanide cluster, a Keggin-type polyoxomolybdate, and PDA (1,10-phenanthroline-2,9-dicarboxylic acid) was prepared and fully characterized by elemental analysis, Fourier-transform infrared and UV–Vis spectroscopies, thermogravimetric analysis, powder X-ray diffraction (PXRD), and single-crystal X-ray diffraction. The structural analysis study showed that the  $[\text{SiMo}_{12}\text{O}_{40}]^{4-}$  ions reside in the interspace between two cationic layers as discrete counterions and are not coordinated to the rare-earth ions. Significantly, this hybrid catalyst is a rare case of an inorganic–organic hybrid polyoxometalate (POM) with a PDA ligand based on CSD search (CSD version 5.40  $\text{m}^2 \text{g}^{-1}$  and 51.3  $\text{m}^2 \text{g}^{-1}$ , respectively). The catalytic activity of the hybrid catalyst was successfully examined in the synthesis of 2-amino-4*H*-chromene derivatives through a multicomponent reaction. A three-component, one-pot reaction involving differently substituted benzaldehydes, resorcinol/ $\alpha$ -naphthol/ $\beta$ -naphthol/4-hydroxycoumarin/3-methyl-4*H*-pyrazole-5(4*H*)-one, and malononitrile or ethyl cyanoacetate in the presence of a catalytic quantity of the aforementioned hybrid catalyst in EtOH/ $\text{H}_2\text{O}$  under reflux condition gave the corresponding highly functionalized 2-amino-4*H*-chromenes in satisfactory yields. The catalyst can be reused several times without appreciable loss in its catalytic activity.

## Highlights

- A mild, simple, convenient, and efficient synthetic strategy was developed for the synthesis of biologically and pharmacologically active products.
- A novel inorganic–organic hybrid,  $2[\text{Dy}_4(\text{PDA})_4(\text{H}_2\text{O})_{11}(\text{SiMo}_{12}\text{O}_{40})] \cdot 7\text{H}_2\text{O}$  denoted as POM@Dy-PDA, based on a lanthanide cluster, a Keggin-type polyoxomolybdate, and PDA (1,10-phenanthroline-2,9-dicarboxylic acid) was synthesized.
- POM@Dy-PDA catalyzed synthesis of 2-amino-4*H*-chromenes via one-pot multicomponent reactions.

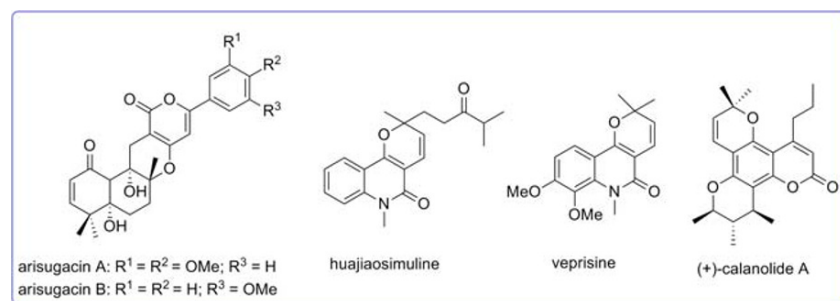
- This protocol is being performed under green conditions, isolating the desired products through facile work-up procedure, in excellent yields.

**KEYWORDS**2-amino-4*H*-chromenes, Heteropoly acids, inorganic–organic hybrid, Keggin, polyoxometalates**1 | INTRODUCTION**

The concept of green chemistry plays a significant role in adapting major scientific encounters to protect our environment. Commonly, the reaction conditions are totally changed, modified, or improved in a way to minimize pollution and side products. Thus, one avoids the use of toxic and volatile organic solvents, performs the reaction at or close to ambient conditions, uses a green heterogeneous catalyst, and if heating is required, one uses unconventional sources of energy such as Microwave irradiation (MWI) or ultrasonic irradiation. If possible, solvent-free conditions should be used to perform useful chemical conversions while minimizing side products and waste material. Thus, the design and preparation of novel green and reusable heterogeneous catalysts to fulfill the principles of green chemistry are still in much demand.<sup>[1,2]</sup> Multicomponent reactions (MCRs) play a significant role in modern synthetic organic chemistry. Their well-established advantages such as atom economy, convergent character, simplicity, and usefulness of a one-pot method, performing the reaction without isolation and purification of intermediates, use of commercially available inexpensive or easily accessible starting materials are quite in agreement with the principles of green chemistry.<sup>[3]</sup> Different heterocyclic systems, for example, benzopyrans, benzoxanthene, and benzochromene have been constructed via one-pot MCRs.<sup>[3]</sup> 4*H*-Pyran derivatives and 4*H*-pyran-annulated heterocyclic moieties, namely, 4*H*-chromene, which are the common framework of various oxygen-containing heterocycles present in natural products have attracted much attention. This structural scaffold is generally present in various kinds of alkaloids exhibiting different pharmacological and biological properties such as antimicrobial and antifungal,<sup>[4]</sup>

anti-inflammatory,<sup>[5]</sup> antitumor,<sup>[6]</sup> anti-HIV,<sup>[7,8]</sup> and antiallergenic<sup>[9,10]</sup> activities, together with antineurodegenerative activity toward disorders including Huntington's diseases, Parkinson's disease, and Alzheimer's disease.<sup>[11,12]</sup> These aspects have attracted the attention of synthetic organic chemists to design and develop analogs of several alkaloids, for example, (+)-calanolide A,<sup>[13]</sup> arisugacin,<sup>[14]</sup> veprisine, and huajiaosimuline,<sup>[15,16]</sup> that all include the main pyran-annulated pharmacophoric scaffold (Figure 1).

2-Amino-4*H*-chromene derivatives are known to be scaffolds of biologically active, naturally occurring compounds,<sup>[17]</sup> thus various approaches for the construction of dihydropyrano[2,3-*c*]chromene derivatives have been developed.<sup>[18–22]</sup> 2-Amino-3-cyano-4*H*-chromene derivatives are commonly synthesized through MCRs involving an appropriate aldehyde, malononitrile (ethyl cyanoacetate),<sup>[23]</sup> and enolizable C–H acids such as barbituric acid, dimedone, resorcinol, naphthol ( $\alpha$  and  $\beta$ ), Kojic acid, and 2-hydroxy-1,4-naphthoquinone-4-hydroxycoumarin in a one-pot fashion. The reaction is assumed to proceed via a Knoevenagel-carba-Michael-Thorpe-Ziegler-type cascade method.<sup>[24]</sup> These MCRs are performed in the presence of diverse heterogeneous or homogeneous catalysts including NaOH,<sup>[25]</sup> TiCl<sub>4</sub>,<sup>[26]</sup> piperidine,<sup>[27]</sup> K<sub>2</sub>CO<sub>3</sub>,<sup>[28]</sup> InCl<sub>3</sub>,<sup>[29]</sup> tetramethylguanidine,<sup>[30]</sup> Et<sub>3</sub>N,<sup>[31]</sup> triethylbenzylammonium chloride,<sup>[32]</sup> cetyltrimethylammonium chloride,<sup>[23]</sup> Preyssler heteropoly acid,<sup>[33]</sup> nano-sized magnesium oxide,<sup>[34]</sup> *N*, *N*-dimethylaminoethylbenzyl dimethylammonium chloride,<sup>[35]</sup> or  $\gamma$ -alumina.<sup>[35]</sup> These approaches have their own merits and drawbacks, and thus the introduction of novel effective heterogeneous and green catalysts is still in much demand. Nowadays, the mainstream of



**FIGURE 1** Selected biologically active compounds containing the pyran-annulated motif

the research has been focused on the preparation of new active catalysts with economic feasibility for being conducted at an industrial level as well as complying with green chemistry principles.<sup>[36,37]</sup> Heteropolyacids (HPAs) and polyoxometalates (POMs) are well-known anionic metal–oxygen clusters with a wide range of sizes, nuclearities, shapes, and varied redox properties. HPAs and POMs have been employed in photochromism, separation, electrochemistry, magnetism, and especially catalysis.<sup>[38–42]</sup> Among the POMs, Keggin-type polyoxomolybdates have recently found many applications.<sup>[43–46]</sup> The application of POMs as catalysts originated from their inherent resistance to oxidative decomposition, high thermal stability, impressive sensitivity to light and electricity,<sup>47</sup> and having different active sites such as protons, oxygen atoms, and metals. The presence of protons and metal ions with unoccupied orbitals give higher acidic character to POMs, which guarantee their catalytic activity especially in acid-catalyzed reactions. In addition, the basic properties of some surface oxygen atoms of POM anions, in particular those on the lacunary sites of lacunary POM anions with a high negative charge, are suitable to be used in base-catalyzed reactions.<sup>[48–52]</sup> POMs have been extensively used as homogeneous catalysts, owing to their good solubility in water and several organic solvents. Although homogenous catalysis is often preferred over heterogeneous catalysis in many organic transformations, they suffer from some drawbacks such as difficulty in separation of the catalyst from the reaction mixture, which hampers their reusability as well as purification of products. Heterogenization of homogeneous catalysts can circumvent the aforementioned problems which are of great importance from economic and environmental points of view in academia and particularly in chemical industries.<sup>[53–55]</sup> By contrast, the specific surface areas of pure bulk POMs are relatively small which prevent accessibility to active sites, thus affecting their catalytic activity. For these reasons, the catalyst engineering of POMs is in much demand. Traditional methods for the catalyst engineering of POMs include increasing their specific surface areas and immobilization of POMs on various porous silica and zeolite supports.<sup>[56,57]</sup> However, the hydrophilic frameworks of the support largely restrict their catalytic activities because of the low accessibility of the active sites for hydrophobic reactants. A promising approach to overcome such problems is the heterogenization of POMs, that is, combination with metal–organic coordination complexes to construct crystalline inorganic–organic hybrids with high-dimensional supramolecular networks. In this way, the high catalytic performance is

achieved by increasing the specific surface area and number of active sites. In addition, synergistic interaction of two moieties in inorganic–organic hybrid compounds results in effective recyclability of heterogeneous catalyst that agrees with the principles of green chemistry.<sup>[58–62]</sup> Hybrid POMs have been studied as catalysts in different reactions such as oxidation of alcohols and carbonyl compounds, alkene polymerization, and the hydrolysis of esters.<sup>[63–68]</sup> For example, Fe(salen)–POM and Co(salen)–POM were successfully used in oxidation of alkanes and primary and secondary benzyl halides. In these transformations, M(salen)–POM gave better yields in shorter reaction times compared with those of its parent, M(salen) complex.<sup>[69,70]</sup>

In the last two decades, our research group has employed HPAs,<sup>[71]</sup> POMs,<sup>[72]</sup> and inorganic–organic hybrids based on PMOs<sup>[73–79]</sup> as highly effective and green homogeneous and heterogeneous catalysts.<sup>[65,80–82]</sup> Among POMs, Keggin-type  $[X_{12}O_{40}]^{n-}$  ions have been mostly employed for constructing inorganic–organic hybrids materials because of their suitable size and structural stability. They can interact with metal–organic complexes through covalent and noncovalent bonds which play an inorganic ligand and a charge-balancing anion role, respectively.<sup>[83,84]</sup> Lanthanoid coordination complexes are particularly valuable in this context because of their Lewis acid properties.<sup>[85–88]</sup> They are hard Lewis acids in which hybridization with POMs increase catalytic activity. They also have a tendency to form bonds with ligands containing hard donor atoms such as oxygen, nitrogen, or fluorine. Expectedly, the suitable selection of metal–organic compounds for combination with POMs gives rise to efficient catalytic properties. Therefore, the logical choice of organic ligand is one of the important points in designing a polymer that can eventually determine the dimensionality of the final solid state structure. One of the best kinds of ligands that require the lowest energy upon complexation to metal ion and that give more thermodynamic stability and greater selectivity without any change in conformation are preorganized ligands.<sup>[89–91]</sup> Phenanthroline ligands with donor groups at the 2- and 9-positions, that is, alcohols, amides, and carboxylates, especially PDA (1,10-phenanthroline-2,9-dicarboxylic acid), are well-known examples of preorganized ligands. Some metal-ion complexing properties of PDA have been reported by Hancock et al.<sup>[92–94]</sup> A CSD search on 1,10-phenanthroline (phen) showed that much research has been done with this ligand (more than 9000 compounds so far). However, according to the CSD, PDA, as an important phen derivative, has just<sup>[64]</sup> compounds, in which there are metal–organic complexes and only four

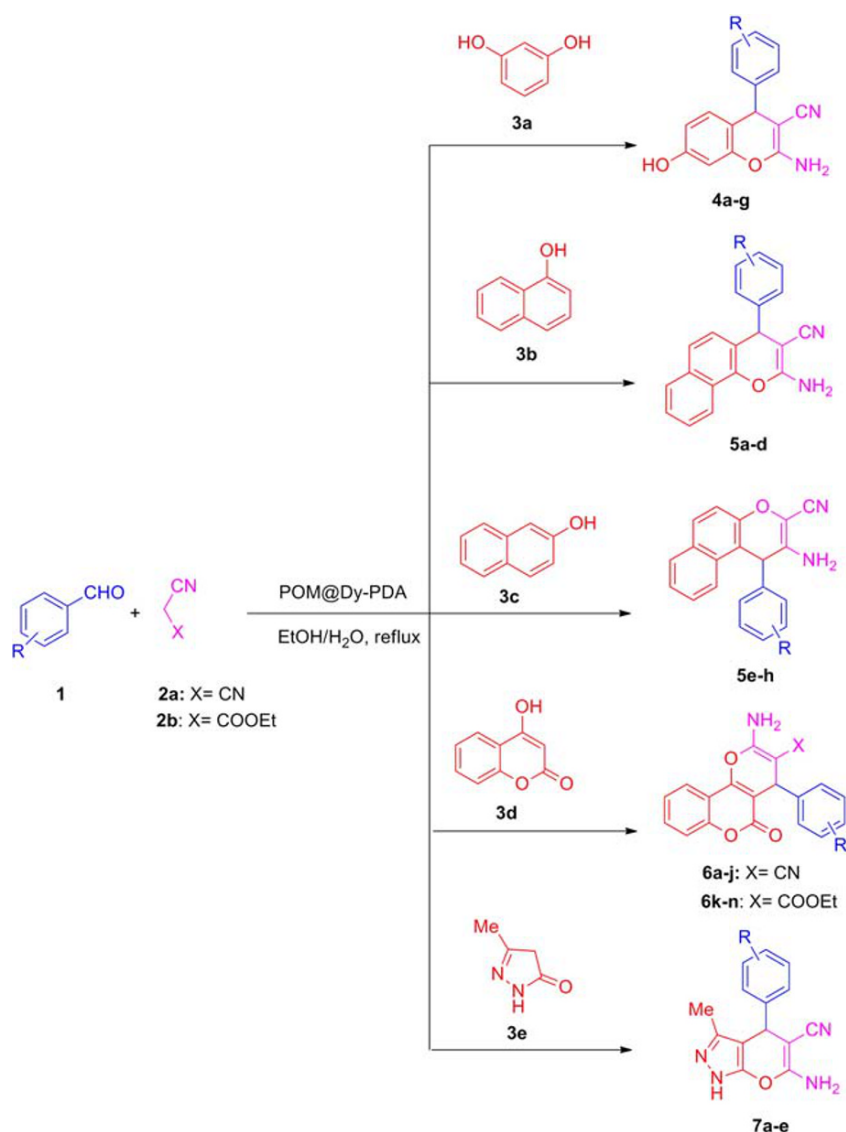
inorganic–organic hybrid architecture based on Keggin-type POMs. Based on the points mentioned earlier, in this article we wish to reveal the preparation of a novel inorganic–organic hybrid catalytic system using PDA as the organic ligand,  $[\text{SiMo}_{12}\text{O}_{40}]^{4-}$  Keggin-type POM as the inorganic building unit, and dysprosium(III) as the lanthanide ion by hydrothermal methods and our successful attempts to examine it as an effective and green catalyst in the synthesis of 2-amino-4*H*-chromenes via MCR. We are interested in heterocyclic chemistry,<sup>[95–98]</sup> particularly in the synthesis of heterocyclic derivatives through MCR<sup>[99–101]</sup> in the presence of heterogeneous catalysts,<sup>[102,103]</sup> especially in the presence of POMs as heteropoly acids (HPAs) and salts of POM. Herein, we describe the synthesis of a novel POM@Dy-PDA as a unique organic–inorganic hybrid, which is fully characterized using Fourier-transform infrared (FT-IR) spectroscopy, elemental analysis, UV–Vis, thermogravimetric analysis (TGA), powder X-ray diffraction (PXRD), and

single-crystal X-ray diffraction. Its catalytic activity was successfully examined in the synthesis of 2-amino-4*H*-chromene derivatives via one-pot, three-component reactions of aromatic aldehydes with resorcinol/ $\alpha$ -naphthol/ $\beta$ -naphthol/4-hydroxycoumarin/3-methyl-4*H*-pyrazole-5 (4*H*)-one, and malononitrile or ethyl cyanoacetate (Scheme 1).

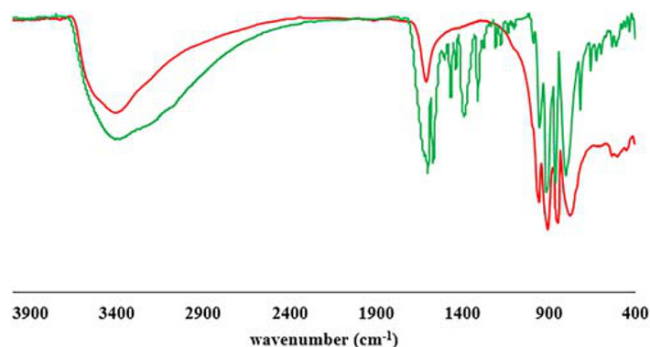
## 2 | EXPERIMENTAL

### 2.1 | Materials

All chemicals were purchased from Merck Company and used as received, except for PDA, which was synthesized according to a reported procedure.<sup>[104]</sup> IR spectra were recorded in KBr pellets in the 4000–400  $\text{cm}^{-1}$  region using a Buck 500 IR and Tensor 27 spectrophotometer. Elemental analysis (CHN) was performed using a

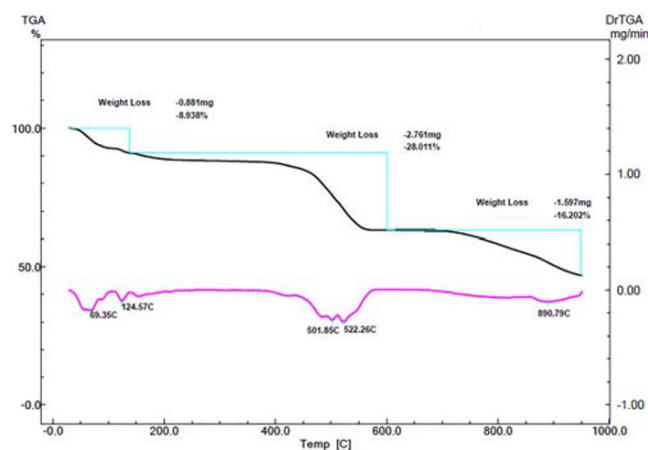


**SCHEME 1** One-pot and three-component synthesis of 2-amino-4*H*-chromenes **5–7** catalyzed by POM@Dy-PDA under reflux condition in EtOH/H<sub>2</sub>O. Dy, dysprosium; PDA, 1,10-phenanthroline-2,9-dicarboxylic acid; POM, polyoxometalate

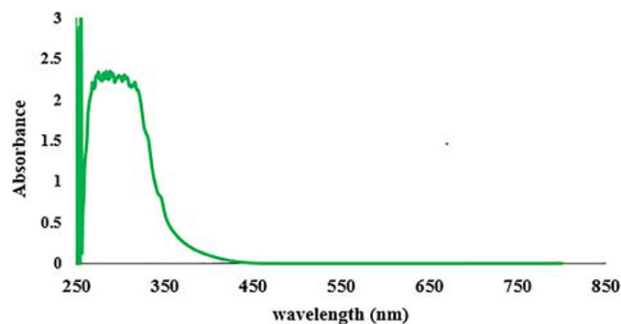


**FIGURE 2** Fourier transform infrared spectrum of POM@Dy-PDA (green) and pure  $[\text{SiMo}_{12}\text{O}_{40}]^{4-}$  (red). Dy, dysprosium; PDA, 1,10-phenanthroline-2,9-dicarboxylic acid; POM, polyoxometalate

Thermo Finnigan Flash-1112EA instrument (German Merck Company). Thermal gravimetric analysis (TGA) was carried out under an air atmosphere from ambient temperature up to 950 °C with a heating rate of 10 °C min<sup>-1</sup> on a Shimadzu TGA-50 instrument. Melting points were measured by an electro thermal 9200 apparatus (German Merck Company). UV-Vis spectroscopy (German Merck Company) was conducted in the wavelength range 200–850 nm using a Perkin Elmer (Lambda 35) spectrophotometer. All products were identified by comparison of their physical (melting points) and spectral (FT-IR spectra) properties with those of authentic samples and found to be identical. The PXRD pattern was recorded with an ASENWAREV (AW-XDM300) (German Merck Company) diffractometer at voltage 45 kv and current 40 mA with Cu- radiation ( $\lambda = 1.54184$  Å). Brunauer–Emmett–Teller (BET) (German Merck Company) surface area analysis was performed using BELSORP-mini II instrument to obtain the nitrogen adsorption–desorption isotherms at 77 K. Samples were



**FIGURE 3** Thermogravimetric analysis (TGA) plots of the POM@Dy-PDA. Dy, dysprosium; PDA, 1,10-phenanthroline-2,9-dicarboxylic acid; POM, polyoxometalate

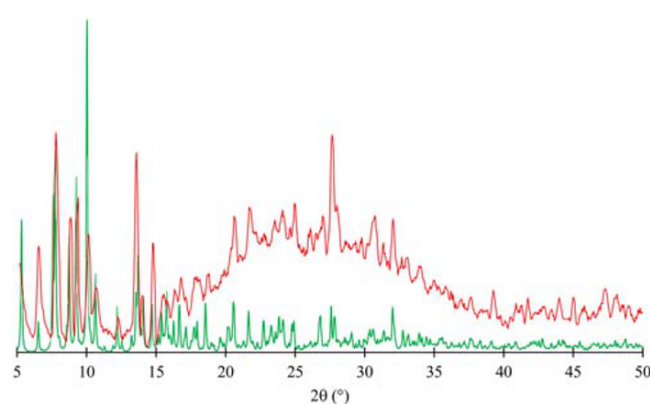


**FIGURE 4** The UV-Vis absorption spectra of the POM@Dy-PDA in dimethyl sulfoxide. Dy, dysprosium; PDA, 1,10-phenanthroline-2,9-dicarboxylic acid; POM, polyoxometalate

degassed under vacuum at 313 K for 24 h. The average pore diameter was calculated using the Barrett–Joyner–Halenda method.

## 2.2 | Synthesis and characterization of $[\text{Dy}_4(\text{PDA})_4(\text{H}_2\text{O})_{11}(\text{SiMo}_{12}\text{O}_{40})] \cdot 7\text{H}_2\text{O}$ hybrid catalyst)POM@Dy-PDA(

A mixture of  $\text{H}_4[\text{SiMo}_{12}\text{O}_{40}] \cdot x\text{H}_2\text{O}$  (182 mg, 0.1 mmol),  $\text{Dy}(\text{NO}_3)_3 \cdot 6\text{H}_2\text{O}$  (109 mg, 0.25 mmol), PDA (67 mg, 0.25 mmol), and deionized water (15 mL) was stirred in air for about 30 min and the pH value was adjusted to about 1.8 with aqueous NaOH (1 M). The mixture was transferred to a Teflon-lined autoclave (30 mL) and kept at 130 °C for 3 days. After slow cooling for 2 days, the solution was filtered off and light yellow crystals were obtained in 51.44% yield (based on Mo). Anal. Calcd. For  $\text{C}_{112}\text{H}_{106}\text{Dy}_8\text{Mo}_{24}\text{N}_{16}\text{O}_{147}\text{Si}_2$ : C 17.50, H 1.39, N 2.92%; found: C 17.16, H 1.62, N 2.94%. IR (KBr pellet,  $\text{cm}^{-1}$ ): 3381, 1600, 1568, 1464, 1389, 1309, 952, 904, 799, 716.



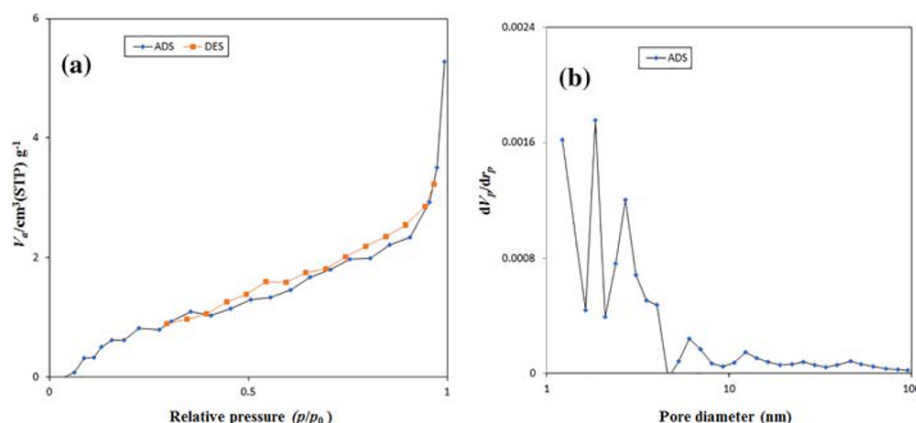
**FIGURE 5** The powder X-ray diffraction pattern of catalyst: green, calculated from single-crystal X-ray data; red, experimental data



## 2.3 | Synthesis of 2-amino-4H-chromenes: General procedure

A mixture of an appropriate benzaldehyde (1 mmol), malononitrile/ethyl cyanoacetate (1 mmol), and 4-hydroxycoumarin/ $\alpha$ / $\beta$ -naphthol/resorcinol/3-methyl-4

*H*-pyrazole-5(4*H*)-one (1 mmol) was refluxed in EtOH/H<sub>2</sub>O (5 mL) in the presence of a catalytic quantity of POM@Dy-PDA (10 mol%) for the indicated reaction time. The progress of the reaction was monitored by thin-layer chromatography (TLC; 7:3 *n*-hexane/ethyl acetate). Upon completion of the reaction (indicated by TLC), the



**FIGURE 6** Nitrogen adsorption (ADS)–desorption (DES) isotherms of POM@Dy-PDA. (b) Pore size distribution curve of POM@Dy-PDA. Dy, dysprosium; PDA, 1,10-phenanthroline-2,9-dicarboxylic acid; POM, polyoxometalate

**TABLE 1** Crystallographic data and refinement details for POM@Dy-PDA

Crystal data	
Chemical formula	$2(\text{C}_{56}\text{H}_{46}\text{Dy}_4\text{N}_8\text{O}_{27}) \cdot 2(\text{Mo}_{12}\text{O}_{40}\text{Si}) \cdot 2.5(\text{H}_2\text{O}) \cdot 4\text{O}$
$M_r$	7716.85
Crystal system, space group	Monoclinic, $P2_1/n$
Temperature (K)	150
$a, b, c$ (Å)	13.258 (3), 23.375 (5), 33.805 (7)
$\beta$ (°)	99.717 (3)
$V$ (Å <sup>3</sup> )	10326(4)
$Z$	2
Radiation type	Mo- $K_\alpha$
$\mu$ (mm <sup>-1</sup> )	4.38
Crystal size (mm)	$0.28 \times 0.19 \times 0.09$
Data collection	
Diffractometer	Bruker Smart APEX CCD
Absorption correction	Multi-scan SADABS
$T_{\min}, T_{\max}$	0.37, 0.69
Number of measured, independent, and observed [ $I > 2\sigma(I)$ ] reflections	198,935; 27,813; 21,088
$R_{\text{int}}$	0.070
$(\sin \theta/\lambda)_{\text{max}}$ (Å <sup>-1</sup> )	0.687
Refinement	
$R[F^2 > 2\sigma(F^2)], wR(F^2), S$	0.070, 0.189, 1.09
Number of reflections	27,813
Number of parameters	1480
Number of restraints	882
H-atom treatment	H-atom parameters constrained
$\Delta\rho_{\text{max}}, \Delta\rho_{\text{min}}$ (e Å <sup>-3</sup> )	8.85, -6.80
CCDC no.	1946762

Computer programs: APEX3 (Bruker, 2016), SAINT (Bruker, 2016), SHELXT (Sheldrick, 2015a), SHELXL-2018/1 (Sheldrick, 2015b), DIAMOND (Brandenburg & Putz, 2012), SHELXTL (Bruker, 2016).

Dy, dysprosium; PDA, 1,10-phenanthroline-2,9-dicarboxylic acid; POM, polyoxometalate.

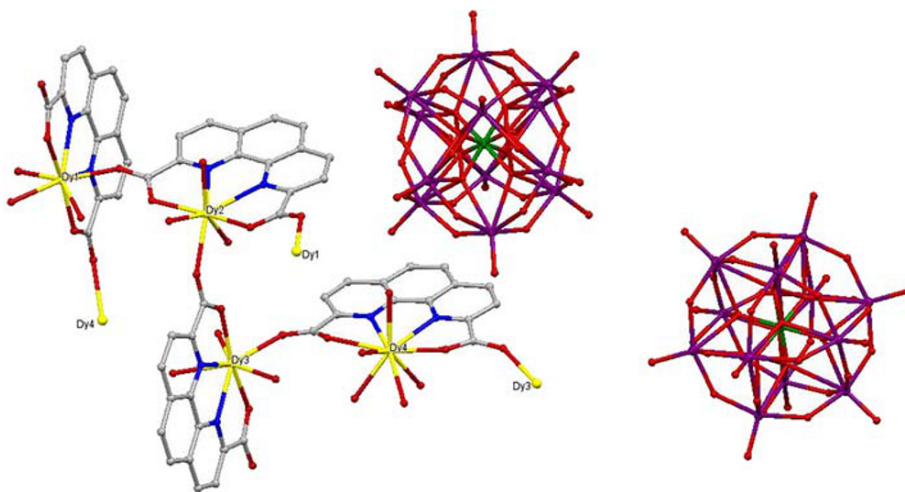
mixture was filtered under reduced pressure. The filtrate was cooled to room temperature and the precipitated solid was separated by filtration under reduced pressure. The anticipated products were purified by crystallization from a mixture of EtOH/H<sub>2</sub>O to give the respective desired products. The products were identified by comparison of their melting points as well as their FT-IR spectra with those of authentic samples (Tables 4–7) (Supporting Information).

### 3 | RESULTS AND DISCUSSION

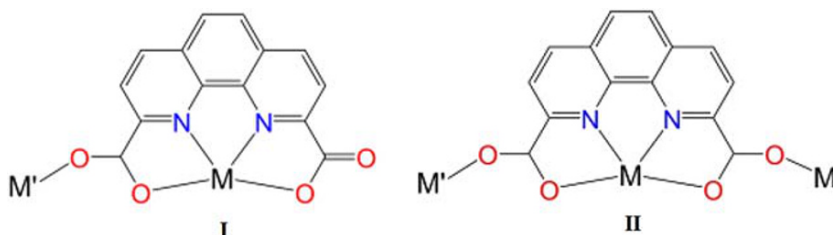
#### 3.1 | Synthesis and characterization of POM@Dy-PDA

The successful synthesis of POM@Dy-PDA was achieved by the hydrothermal reaction of lanthanide nitrate, organic ligand, and H<sub>4</sub>SiMo<sub>12</sub>O<sub>40</sub>·xH<sub>2</sub>O as the inorganic building unit. The applied reaction conditions such as

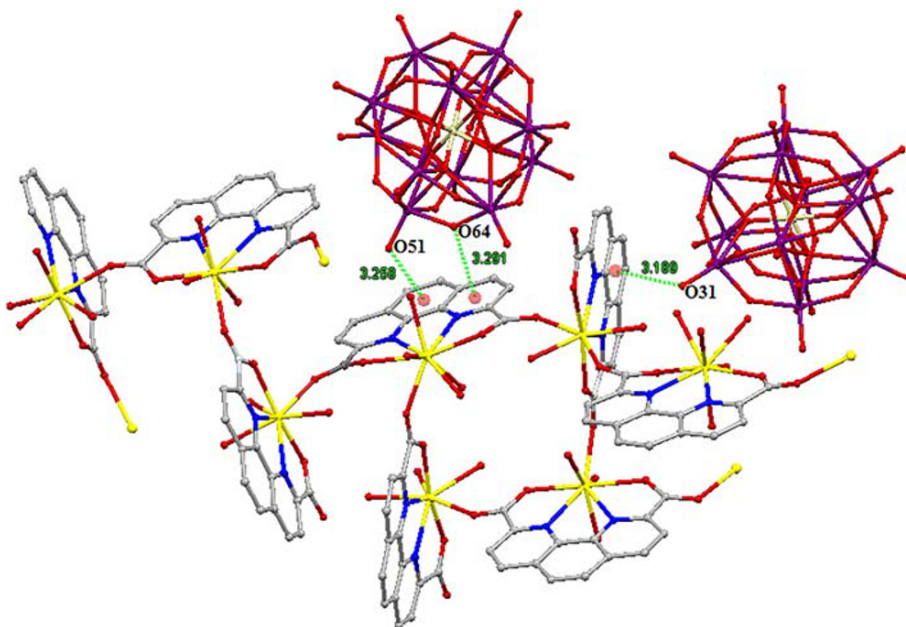
**FIGURE 7** A view of the molecular structure of POM@Dy-PDA. Interstitial water molecules and H atoms have been omitted for clarity. Color code: Dy, yellow; O, red; Mo, purple; N, blue; Si, green; and C, gray. Dy, dysprosium; PDA, 1,10-phenanthroline-2,9-dicarboxylic acid; POM, polyoxometalate



**FIGURE 8** Coordination modes found for the PDA ligand in the POM@Dy-PDA. The ligands chelating Dy1, Dy3 are found in mode I and for ligands chelating Dy2, Dy4 mode II is found



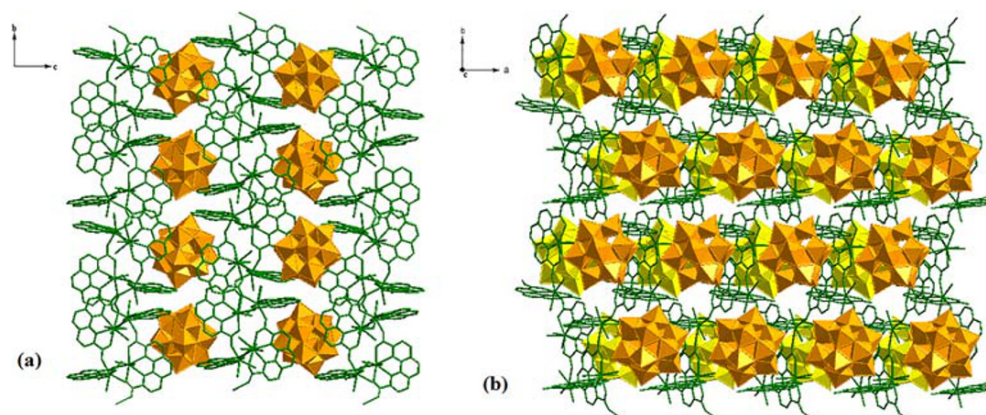
**FIGURE 9** Partial view of the crystal packing of POM@Dy-PDA showing the intermolecular anion–interactions (in Å) established between the organic ligand and atoms O51, O64, and O31 of the Keggin counterpart. Color code: Dy, yellow; O, red; Mo, purple; N, blue; Si, green; and C, gray. Dy, dysprosium; PDA, 1,10-phenanthroline-2,9-dicarboxylic acid; POM, polyoxometalate



temperature, pH value, and molar ratio of reactants have been optimized. The mixture was stirred in air for 30 min. Finally, the pH was adjusted to approximately 1.8 with aqueous NaOH solution. The mixture was transferred to a Teflon-lined autoclave and kept at 130 °C for 3 days. After slow cooling for 2 days, the solution was filtered off and light yellow crystals were obtained. Anal. Calcd. For POM@Dy-PDA: C 17.50, H 1.39, N 2.92%; found: C 17.16, H 1.62, N 2.94%, which show that the results of the analysis are in good agreement with calculated values.

The FT-IR spectra of POM@Dy-PDA and  $[\text{SiMo}_{12}\text{O}_{40}]^{4-}$  Keggin are shown in Figure 2. The presence of the Keggin-type  $[\text{SiMo}_{12}\text{O}_{40}]^{4-}$  anions is confirmed by the characteristic pattern in the region below  $1000\text{ cm}^{-1}$ . Four bands are attributed to  $\nu(\text{Si}-\text{O}_a)$ ,  $\nu(\text{Mo}=\text{O}_t)$ ,  $\nu(\text{Mo}-\text{O}_b)$ , and  $\nu(\text{Mo}-\text{O}_c)$  stretching vibrations, which appear at an average of 952, 904, 860, and  $798\text{ cm}^{-1}$ , respectively (where  $\text{O}_t$  is a terminal oxygen,  $\text{O}_b$

is a bridging oxygen,  $\text{O}_a$  is an internal oxygen, and  $\text{O}_c$  is a bridging oxygen within the edge-sharing octahedra).<sup>[105]</sup> Compared with the typical parent anion in  $[\text{SiMo}_{12}\text{O}_{40}]^{4-}$ , the vibrational frequencies related to the terminal oxide groups ( $\text{Mo}=\text{O}_t$ ) and ( $\text{Mo}-\text{O}_b$ ) are red shifted. This shows that the terminal ( $\text{O}_t$ ) and bridge ( $\text{O}_b$ ) oxygen atoms are most affected by hydrogen bonding with water molecules.<sup>[106]</sup> The characteristic pattern in the region  $1000\text{--}1621\text{ cm}^{-1}$  can be attributed to the coordinated PDA ligands. The absence of  $\nu(\text{C}=\text{O})$  stretching vibrations at  $1700\text{--}1720\text{ cm}^{-1}$  demonstrates the complete deprotonation of the carboxylic groups in the PDA ligands. Strong asymmetric and symmetric stretching frequencies for the carboxylate groups appear at 1600 and  $1389\text{ cm}^{-1}$ , respectively. The bands resulting from the vibrations of the aromatic skeleton also appear at  $1464\text{ cm}^{-1}$ . The band centered at  $3381\text{ cm}^{-1}$  is attributed to the  $\nu(\text{OH})$  vibrations of the lattice and coordinated water molecules.



**FIGURE 10** (a) A polyhedral view of the 2D supramolecular sheet in POM@Dy-PDA. (b) A polyhedral view of the 3D supramolecular framework of hybrid catalyst. (Note: Only for more clarity, in b, Mo atoms are represented in two different colored polyhedra). Dy, dysprosium; POM, polyoxometalate

**TABLE 2** Selected bond lengths (Å) of POM@Dy-PDA

Dy1-O6	2.276 (7)	Dy2-O8	2.354 (7)	Dy4-O2 <sup>[iii]</sup>	2.356 (9)
Dy1-O3	2.325 (8)	Dy2-O7	2.378 (8)	Dy4-O25	2.377 (9)
Dy1-O77 <sup>[i]</sup>	2.341 (7)	Dy2-O13	2.384 (6)	Dy4-O23	2.384 (9)
Dy1-O1	2.356 (8)	Dy2-N3	2.495 (7)	Dy4-O21	2.388 (8)
Dy1-O9 <sup>[ii]</sup>	2.382 (7)	Dy2-N4	2.519 (7)	Dy4-O26	2.402 (9)
Dy1-O5	2.400 (8)	Dy3-O19	2.343 (7)	Dy4-O20	2.466 (8)
Dy1-N2	2.468 (8)	Dy3-O15	2.346 (7)	Dy4-O24	2.494 (12)
Dy1-N1	2.485 (8)	Dy3-O17	2.350 (7)	Dy4-N7	2.512 (7)
Dy2-O10	2.308 (8)	Dy3-O18	2.371 (7)	Dy4-N8	2.540 (7)
Dy2-O12	2.346 (7)	Dy3-O14	2.376 (6)	Dy4-O2 <sup>[iii]</sup>	2.356 (9)
Dy2-O11	2.354 (9)	Dy3-N5	2.479 (7)	Dy4-O25	2.377 (9)

Symmetry codes:

<sup>i</sup>—  $x + 3/2, y + 1/2, -z + 1/2$ ;

<sup>ii</sup>—  $x + 1/2, y + 1/2, -z + 1/2$ ;

<sup>iii</sup>—  $x + 3/2, y - 1/2, -z + 1/2$ .

Dy, dysprosium; PDA, 1,10-phenanthroline-2,9-dicarboxylic acid; POM, polyoxometalate.



To investigate the thermal stabilities of the POM@Dy-PDA, TGA experiments were carried out under an air atmosphere from 20 to 950 °C. The TGA curve exhibits three main stages. The first weight loss of 8.93% (calcd. 8.50%) occurred in the temperature range of 25–140 °C and corresponds to the loss of all lattice and coordinated water molecules. The second weight loss of 28.01% between 140 and 600 °C (calcd. 27.93%) is assigned to the loss of the four PDA ligands. The third step between 600 and 900 °C with a loss of 16.20% (calcd. 16.26%) can be attributed to the loss of  $\text{Mo}_2\text{O}_5 + 2\text{MoO}_2 + \text{SiO}_4$ . After the thermal decomposition of POM@Dy-PDA, 53.151% of its initial weight remained (Figure 3).

The UV–Vis absorption spectrum of the POM@Dy-PDA is shown in Figure 4. In the ultraviolet region (200–400 nm), there are three absorption bands at 318, 328, and 347 nm, which are assigned to ligand-to-metal charge transfer for the POM. This represents the transfer of an electron from the highest occupied molecular orbital to the lowest unoccupied molecular orbital.<sup>[107]</sup>

As shown in Figure 5, the hybrid catalyst was characterized via PXRD pattern at room temperature. The PXRD pattern measured for the synthesized sample was in good agreement with the PXRD pattern simulated from the respective single-crystal X-ray data, which indicates the good phase purity of the catalyst.

The BET specific surface area and porous structure of the POM@Dy-PDA catalyst was characterized by nitrogen adsorption experiments. As shown in Figure 6, the adsorption–desorption behavior of POM@Dy-PDA shows a type IV isotherm (according to IUPAC classification)

with a clear H3-type hysteresis loop in the relative pressure  $P/P_0$  between 0.4 and 0.94, indicating the formation of mesoporous materials. It is worth mentioning that the BET surface area measured for this catalyst shows a 60% improvement from 4 m<sup>2</sup> g<sup>−1</sup> for commercial  $\text{H}_4\text{SiMo}_{12}\text{O}_{40}$ <sup>[108]</sup> to 6.6 m<sup>2</sup> g<sup>−1</sup> for POM@Dy-PDA (Langmuir surface area of 51.3 m<sup>2</sup> g<sup>−1</sup>) after hybridization. However, pore-size analysis with the Barrett–Joyner–Halenda (BJH) method revealed a heterogeneous structure.

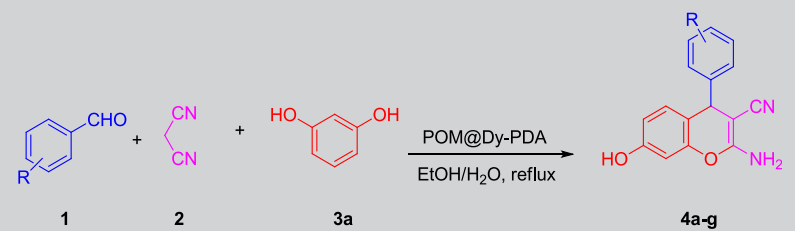
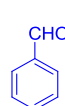
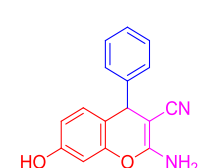
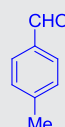
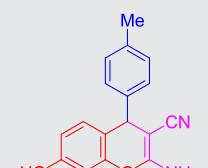
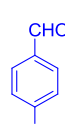
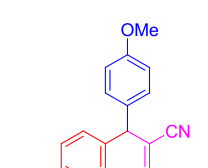
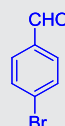
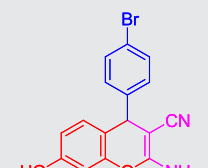
### 3.2 | Crystal structures of the hybrid catalyst (POM@Dy-PDA)

The X-ray structure determination established that the POM@Dy-PDA crystallizes in the monoclinic space group  $P2_1/n$ . Crystallographic and refinement data for the hybrid catalyst are listed in Table 1. The crystal structure of the catalyst contains a polynuclear cation unit  $[\text{Dy}_4(\text{PDA})_4(\text{H}_2\text{O})_{11}]^{4+}$ , two  $[\text{SiMo}_{12}\text{O}_{40}]^{4-}$  polyoxoanions, and seven lattice water molecules (Figure 7). The polyoxoanion  $[\text{SiMo}_{12}\text{O}_{40}]^{4-}$  ion exhibits the well-known Keggin-type structure and is constructed from one  $\text{SiO}_4$  unit and four trimetallic  $(\text{MoO}_6)_3$  groups. The central Si atom sits on a crystallographic center and is surrounded by a distorted cube of eight half-occupied (disordered over the center) oxygen atoms. This type of disorder often appears in the Keggin structure.<sup>[109]</sup> In the cationic component, all Dy(III) ions are crystallographically independent and the  $\text{Dy}^{3+}$  ions are bridged by carboxylate oxygen atoms belonging to four carboxylic acids. The dysprosium(III) ions are eight and nine

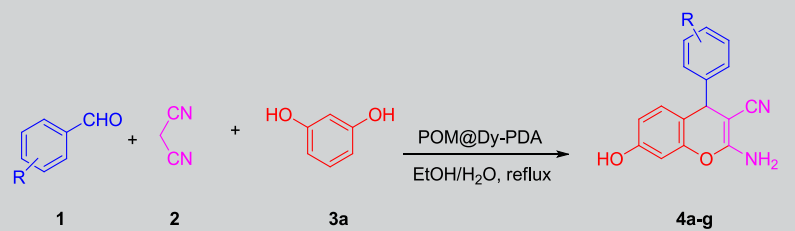
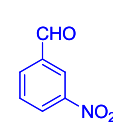
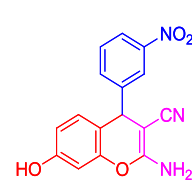
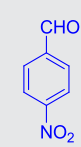
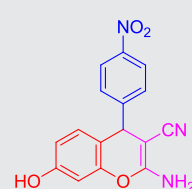
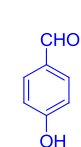
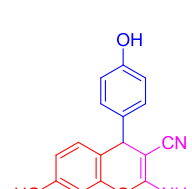
**TABLE 3** Optimization of reaction conditions for the synthesis of 2-amino-4H-chromene **4a**

Entry	Solvent	Temperature	Time (min)	Catalyst amount (mol%)	Yield (%)
1	EtOH/H <sub>2</sub> O	Room temperature	80	–	0
2	EtOH/H <sub>2</sub> O	Reflux	80	No catalyst	Trace
3	MeOH	Reflux	60	10	70
4	CH <sub>2</sub> Cl <sub>2</sub>	Reflux	70	10	52
5	Dimethylformamide	Reflux	60	10	45
6	CH <sub>3</sub> CN	Reflux	60	10	40
7	EtOH	Reflux	60	10	83
8	H <sub>2</sub> O	Reflux	60	10	73
9	EtOH/H <sub>2</sub> O	Reflux	15	10	95
10	EtOH/H <sub>2</sub> O	Room temperature	80	10	35
11	EtOH/H <sub>2</sub> O	Reflux	80	5	35
12	EtOH/H <sub>2</sub> O	Reflux	15	10	95
13	EtOH/H <sub>2</sub> O	Reflux	60	15	95

**TABLE 4** Synthesis of 2-amino-3-cyano-7-hydroxy-4-(aryl)-4*H*-chromene derivatives **4a–g** catalyzed by POM@Dy-PDA

						
Entry	Aldehyde	Product	Time (min)	Yield (%)	Observed MP (°C)	Literature MP (°C)
1		 <b>4a</b>	15	95	229–232	231–233 <sup>[110]</sup>
2		 <b>4b</b>	18	91	186–188	185–187 <sup>[110]</sup>
3		 <b>4c</b>	18	90	190–193	192–194 <sup>[111]</sup>
4		 <b>4d</b>	20	92	232–234	233–235 <sup>[110]</sup>

**TABLE 4** (Continued)

						
Entry	Aldehyde	Product	Time (min)	Yield (%)	Observed MP (°C)	Literature MP (°C)
5			25	85	171–173	170–172 <sup>[110]</sup>
6			20	88	211–213	212–214 <sup>[111]</sup>
7			20	88	247–251	248–250 <sup>[112]</sup>

Dy, dysprosium; MP, melting point; PDA, 1,10-phenanthroline-2,9-dicarboxylic acid; POM, polyoxometalate.

coordinate with DyN<sub>2</sub>O<sub>6</sub> (Dy1, Dy2, and Dy3) and DyN<sub>2</sub>O<sub>7</sub> (Dy4) coordination environments, Dy-N<sub>PDA</sub>: 2.468(8)–2.540(7), Dy-O<sub>PDA</sub>: 2.325(8)–2.466(8), Dy-O<sub>water</sub>: 2.308(8)–2.494(12) Å. It should be noted that all Dy(III) ions are coordinated by PDA ligands and each PDA acts as a chelating and a bridging ligand between two neighboring metal centers. Two different coordination modes of the PDA ligand in POM@Dy-PDA are shown in Figure 8. The ligands chelating Dy1 and Dy3 are found in mode **I** and for ligands chelating Dy2 and Dy4 mode **II** is found.

As shown in Figure 9, the terminal O51 and bridging O64 atoms of the Keggin moieties and also the bridging O31 atoms of another Keggin are oriented toward the  $\pi$  face of one of the phen rings of a neighboring unit. The distances between the O51, O64, and O31 atoms and the centroid of the phen rings are 3.258, 3.291, and 3.189 Å, respectively, which are in the range of typical anion- $\pi$  contacts, and thus a clear indication of binding. This interaction can be also viewed as a lone pair- $\pi$  interaction in which one free lone pair of O51, O64, and O31 atoms points toward

**TABLE 5** Synthesis of 2-amino-benzochromene derivatives **5a–h** catalyzed by POM@Dy-PDA

Entry	Aldehyde	$\alpha$ -Naphthol or $\beta$ -naphthol	Product	Time (min)	Yield (%)	Observed MP ( $^{\circ}\text{C}$ )	Literature MP ( $^{\circ}\text{C}$ )
1				20	90	216–218	216–217 <sup>[113]</sup>
2				25	83	239–241	240–241 <sup>[114]</sup>
3				25	86	231–233	230–232 <sup>[34]</sup>
4				20	92	230–233	231–234 <sup>[34]</sup>
5				18	90	280–283	279–281 <sup>[115]</sup>



TABLE 5 (Continued)

Entry	Aldehyde	α-Naphthol or β-naphthol	Product	Time (min)	Yield (%)	Observed MP (°C)	Literature MP (°C)
6				25	89	239–241	238–240 <sup>[33]</sup>
7				20	90	206–207	205–206 <sup>[116]</sup>
8				20	88	185–187	186–187 <sup>[116]</sup>

Dy, dysprosium; MP, melting point; PDA, 1,10-phenanthroline-2,9-dicarboxylic acid; POM, polyoxometalate.

the  $\pi$ -face of the phen system that is coordinated to the metal, thus enhancing its  $\pi$  acidity.

The overall structure of POM@Dy-PDA is best described as composed of two cationic layers of dysprosium(III) complexes in the crystallographic *bc* plane which are stacked along the *a* axis (Figure 10a). In this compound the POM units reside in the spaces between two adjacent layers as discrete counterions and do not show any coordinating behavior toward the dysprosium ions. It is worth mentioning that the existence

of abundant intermolecular hydrogen bonding supports the 2D sheet structure. Furthermore, extensive hydrogen bonding between surface oxygen atoms of the Keggin anion and neighboring layers and anion- $\pi$  interactions bind the discrete molecules into a 3D supramolecular framework (Figure 10b). The lattice water molecules reside as guests in the interstices of the 3D supramolecular framework through extensive hydrogen-bonding interactions. All of these contacts are given in Table 2.

**TABLE 6** Synthesis of 2-amino-3,4-dihydropyrano[3,2-c]chromene **6a–k** catalyzed by POM@Dy-PDA

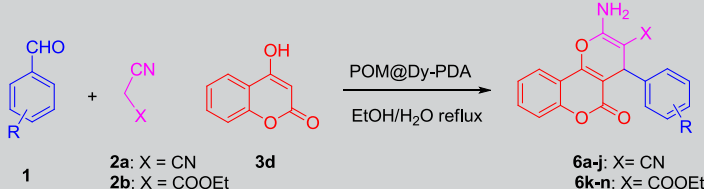
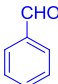

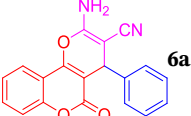
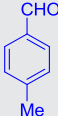
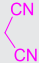
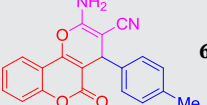
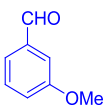

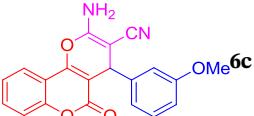
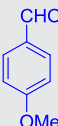

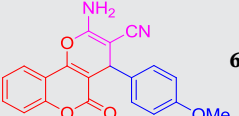
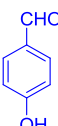

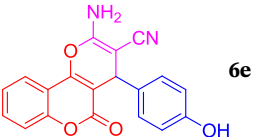
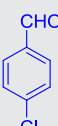

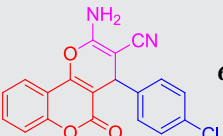
							
Entry	Aldehyde	Malononitrile/ethyl cyanoacetate X = CN/COOEt	Product	Time (min)	Yield (%)	Observed MP (°C)	Literature MP (°C)
1				8	97	255–259	256–258 <sup>[117]</sup>
2				15	91	252–255	253–256 <sup>[117]</sup>
3				18	90	241–243	242–244 <sup>[118]</sup>
4				15	92	248–251	248–250 <sup>[117]</sup>
5				12	94	258–262	259–261 <sup>[119]</sup>
6				10	96	261–263	260–262 <sup>[117]</sup>

TABLE 6 (Continued)

Entry	Aldehyde	Malononitrile/ethyl cyanoacetate X = CN/COOEt	Product	Time (min)	Yield (%)	Observed MP (°C)	Literature MP (°C)
7				15	93	253–255	252–254 <sup>[120]</sup>
8				20	90	256–258	257–259 <sup>[21]</sup>
9				18	92	259–262	260–262 <sup>[121]</sup>
10				12	95	256–259	256–258 <sup>[117]</sup>
11				20	91	209–212	210–212 <sup>[122]</sup>
12				20	88	200–202	199–201 <sup>[123]</sup>
14				18	86	193–195	192–194 <sup>[118]</sup>

(Continues)

TABLE 6 (Continued)

Entry	Aldehyde	Malononitrile/ethyl cyanoacetate X = CN/COOEt	Product	Time (min)	Yield (%)	Observed MP (°C)	Literature MP (°C)
15				15	90	232–235	232–234 <sup>[123]</sup>

Dy, dysprosium; MP, melting point; PDA, 1,10-phenanthroline-2,9-dicarboxylic acid; POM, polyoxometalate.

### 3.3 | Catalytic activity

Considering POM@Dy-PDA, as an ecofriendly inorganic–organic hybrid, after its full characterization, we decided to examine its catalytic activity in the synthesis of 2-amino-4*H*-chromenes through a one-pot MCR. For this purpose, we selected a three-component reaction, involving benzaldehyde **1a**, malononitrile **2a**, and resorcinol **3a** as model reaction (Scheme 1). Initially, we examined the model reaction in the absence of any catalyst or additive by just refluxing the starting materials in EtOH. The reaction was monitored by TLC using *n*-hexane: ethyl acetate (7:3), which showed no conversion. Next, the reaction was conducted in the presence of catalytic amount of freshly prepared POM@Dy-PDA in refluxing ethanol. This reaction was monitored by TLC, showing consumption of starting materials along with formation of a new product which was identified as the corresponding 2-amino-4*H*-chromene **4a**. For the selection of the best solvent, the reaction was conducted in different solvents such as H<sub>2</sub>O, EtOH, MeOH, CH<sub>2</sub>Cl<sub>2</sub>, MeCN, dimethylformamide, and EtOH/H<sub>2</sub>O. The mixture EtOH/H<sub>2</sub>O was found to be the solvent of choice in terms of yield of the product and reaction time. To

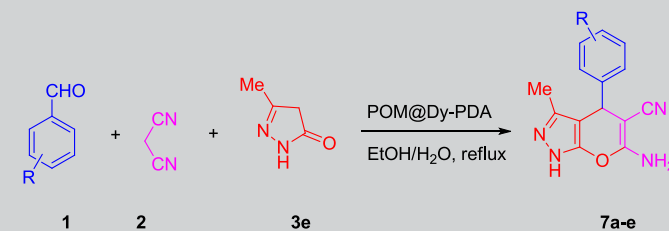
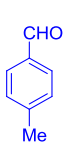
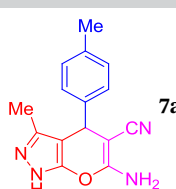
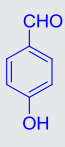
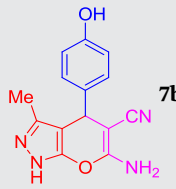
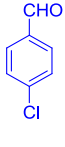
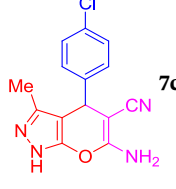
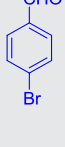
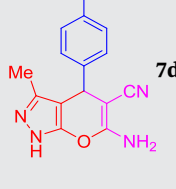
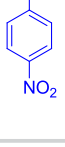
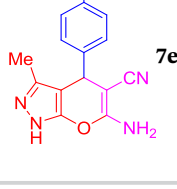
optimize the catalyst loading, we performed the same reaction in the presence of varying quantity of catalyst in EtOH/H<sub>2</sub>O under reflux condition. From Table 3, it can be concluded that 10 mol% of POM@Dy-PDA is the required quantity of catalyst which gave 95% yield of **4a** in 15 min.

Based on the optimal reaction conditions, we investigated the substrate scope of our strategy by using differently substituted benzaldehydes (comprising electron-donating and electron-withdrawing substituents) which were reacted with malononitrile and resorcinol to give the corresponding 2-amino-3-cyano-7-hydroxy-4-(aryl)-4*H*-chromene derivatives **4a–g** in high yields (Table 4). The products were characterized by comparison of their melting points and FT-IR spectra with those of authentic compounds and were found being identical. As shown in Table 4, no noticeable substituent influence was observed. Thus, in general POM@Dy-PDA can be considered as a tolerant, very flexible catalyst for the aforementioned one-pot three-component reaction.

Subsequently, the strategy was extended for the synthesis of a series of 2-amino-4*H*-benzo[*h*]chromene-3-carbonitrile **5a–d**. Accordingly, differently substituted benzaldehydes (bearing electron-withdrawing groups as



**TABLE 7** Synthesis of 2-amino-4*H*-chromene derivatives **7a–e** catalyzed by POM@Dy-PDA

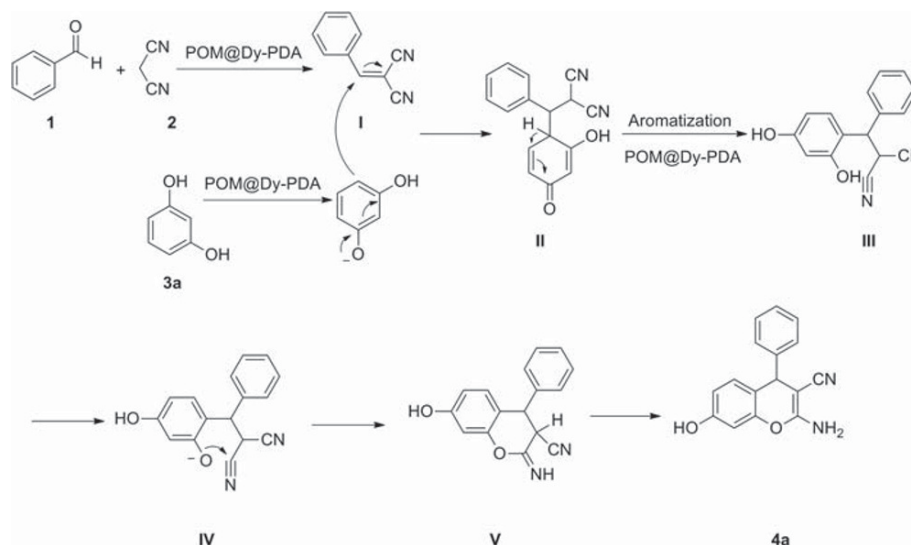
						
Entry	Aldehyde	Product	Time (min)	Yield (%)	Observed MP (°C)	Literature MP (°C)
1			15	93	176–177	175–176 <sup>[124]</sup>
2			20	91	223–225	223–224 <sup>[125]</sup>
3			18	90	233–235	234–236 <sup>[125]</sup>
4			20	85	179–181	178–180 <sup>[125]</sup>
5			20	88	247–250	248–250 <sup>[125]</sup>

Dy, dysprosium; MP, melting point; PDA, 1,10-phenanthroline-2,9-dicarboxylic acid; POM, polyoxometalate.

**TABLE 8** The catalytic activity of POM with POM@Dy-PDA

Entry	R <sup>1</sup>	Carbonyl compound 3	Malononitrile 2a	Product 4	Catalyst	Yield (%)	Time (min)
1	H	<b>3a</b>	<b>2a</b>	<b>4a</b>	POM@Dy-PDA	95	60
2	H	<b>3a</b>	<b>2a</b>	<b>4a</b>	POM	40	180

Dy, dysprosium; PDA, 1,10-phenanthroline-2,9-dicarboxylic acid; POM, polyoxometalate.



**SCHEME 2** A reasonable reaction mechanism for the synthesis of 2-amino-4H-chromenes catalyzed by POM@Dy-PDA. Dy, dysprosium; PDA, 1,10-phenanthroline-2,9-dicarboxylic acid; POM, polyoxometalate

well as electron-donating groups) were reacted with malononitrile and 2-naphthol in the presence of a catalytic amount of POM@Dy-PDA in refluxing EtOH/H<sub>2</sub>O. In all cases, the respective products **5a–d** were obtained in satisfactory yields (Table 5). Accordingly, replacement of the 2-naphthol with 1-naphthol fruitfully gave the corresponding 2-amino-4H-benzo[*h*]chromenes **5a–h** (Table 5).

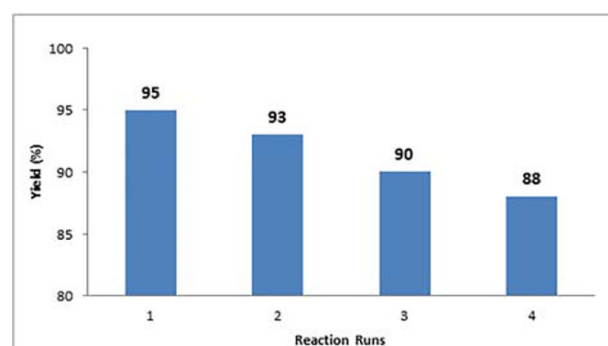
Encouraged by these results, the POM@Dy-PDA-catalyzed synthesis of another important class of chromene-annulated heterocycles, so-called 2-amino-3,4-dihydropyrano[3,2-*c*]chromene **6a–k**, was successfully attempted. Three-component reactions of differently substituted benzaldehydes, 4-hydroxycoumarin, and malononitrile in the presence of 10 mol% POM@Dy-PDA in refluxing EtOH/H<sub>2</sub>O gave the corresponding 2-amino-3,4-dihydropyrano[3,2-*c*]chromene **6a–k** in excellent yields (Table 6). To study the substrate scope of the reaction differently substituted benzaldehydes having electron-releasing or electron-withdrawing substituents such as Me, NO<sub>2</sub>, and OMe were successfully reacted with malononitrile and 4-hydroxycoumarin under the same reaction conditions. The reactions proceeded smoothly to give the products in satisfactory yields. Likewise, the reaction of differently substituted aldehydes with ethyl cyanoacetate and 4-hydroxycoumarin was performed under the similar reaction conditions and the corresponding products were also obtained in satisfactory yields (Table 6).

In further work, the substrate scope and limitations of the preparation of other 2-amino-4H-chromene derivatives in the presence of POM@Dy-PDA was examined. In this study, 3-methyl-4H-pyrazole-5(4H)-one was employed instead of 4-hydroxycoumarin. The generality of this strategy was examined using differently substituted benzaldehydes having either electron-

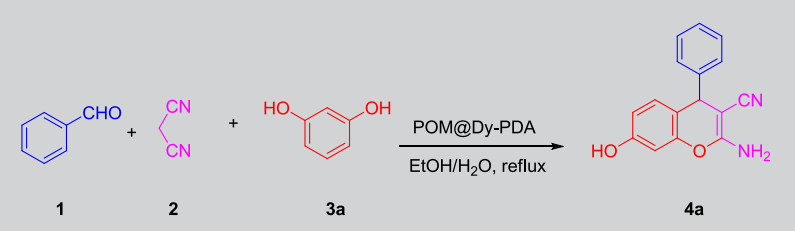
withdrawing or electron-releasing groups in the *ortho*, *meta*, and *para* positions with malononitrile and 3-methyl-4H-pyrazole-5(4H)-one. In all cases the respective 2-amino-4H-chromenes were obtained in satisfactory yields in relatively short times without the formation of any by-products. The results are outlined in Table 7. As can be seen, benzaldehydes bearing electron-donating groups as well as electron-withdrawing moieties could be successfully employed as substrates.

To expand our investigation, we compared the catalytic activity of the commercially available POM [SiMo<sub>12</sub>O<sub>40</sub>]<sup>4−</sup> with that of our POM@Dy-PDA catalyst. For this purpose, the model reaction was conducted in the presence of either [SiMo<sub>12</sub>O<sub>40</sub>]<sup>4−</sup> or POM@Dy-PDA as catalyst in EtOH/H<sub>2</sub>O under reflux condition. The results are outlined in Table 8. The results showed that the POM@Dy-PDA exhibited better catalytic activity compared with [SiMo<sub>12</sub>O<sub>40</sub>]<sup>4−</sup>.

A reasonable reaction mechanism for the catalytic activity of POM@Dy-PDA is suggested based on the literature and our experimental results. It is assumed that the reaction proceeds via a Knoevenagel condensation



**FIGURE 11** Recyclability of catalyst for the synthesis of 2-amino-4H-chromene **4a**

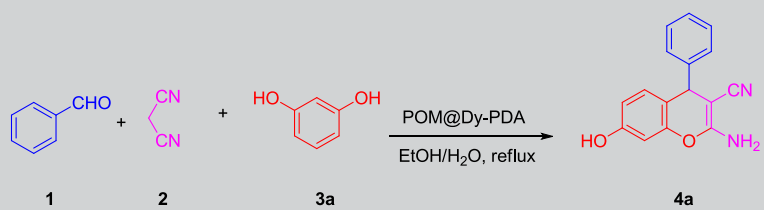
**TABLE 9** The comparison of the catalytic activity of POM@Dy-PDA with formerly reported catalysts for the synthesis of 2-amino-4*H*-chromenes **4a**


The reaction scheme shows the synthesis of 2-amino-4*H*-chromene (**4a**) from benzaldehyde (**1**), malononitrile (**2**), and resorcinol (**3a**). The reaction is catalyzed by POM@Dy-PDA in EtOH/H<sub>2</sub>O at reflux.

Entry	Catalyst	Time	Catalyst Amount	Temperature	Solvent	Yield (%)	Reference
1	No catalyst	5 h	–	Reflux	2,2,2-Trifluoroethanol	90	[138]
2	Potassium phthalimide- <i>N</i> -oxyl	20 min	1.5 mol%	Reflux	H <sub>2</sub> O	90	[126]
3	Mg/Al hydrotalcite	4 h	15 wt%	60 °C	H <sub>2</sub> O	95	[112]
4	Tungstic acid functionalized mesoporous SBA-15	12 h	30 mg	100 °C	H <sub>2</sub> O	86	[127]
5	Nanozeolite clinoptilolite	15 min	0.01 g	Reflux	H <sub>2</sub> O	92	[128]
6	Potassium phthalimide	17 min	9.2 mg (5 mol%)	Ball milling technique RT	–	97	[129]
7	Anhydrous sodium carbonate	10 min	11 mg (10 mol%)	125 °C	Solvent free	>99	[130]
8	A triazine-based porous organic polymer (TPOP-2)	5 h	40 mg	80 °C	Solvent free	87	[131]
9	Ionic liquid, namely, 2-ethyl imidazolium acetate ([2-Eim] OAc)	27 min	10 mol%	67.5 °C	Solvent free	92	[110]
10	Fe <sub>3</sub> O <sub>4</sub> –chitosan nanoparticles (Fe <sub>3</sub> O <sub>4</sub> –chitosan magnetic nanoparticles)	20 min	0.15 g (30 mol%)	Ultrasound irradiation 50 °C	H <sub>2</sub> O	99	[132]
11	Amino-appended β-cyclodextrins	5 h	5 mol% (0.05 mol)	RT	H <sub>2</sub> O	95	[133]
12	Sulfonic acid-functionalized MIL-101(Cr) [MIL-101(Cr)–SO <sub>3</sub> H]	3 h	0.37 mol%	100 °C	H <sub>2</sub> O	82	[134]
13	Imidazolium ionic liquid-functionalized magnetic multiwalled carbon nanotubes (CNTs–Fe <sub>3</sub> O <sub>4</sub> –IL)	5 min	0.020 g	MW 70 °C	H <sub>2</sub> O	97	[135]
14	Monodisperse palladium nanoparticles supported with graphene oxide (Pd@GO)	15 min	10 mg	80 °C	EtOH	92	[136]
15	Palladium–ruthenium nanoparticles decorated on graphene oxide (PdRu@GO)	12 min	8 mg	80 °C	H <sub>2</sub> O/EtOH	95	[111]
16	–	1 min	–	Ultrasonic conditions 60 °C	H <sub>2</sub> O	98	[139]

(Continues)

TABLE 9 (Continued)



Entry	Catalyst	Time	Catalyst Amount	Temperature	Solvent	Yield (%)	Reference
17	Fe <sub>3</sub> O <sub>4</sub> @SiO <sub>2</sub> -Benzim-Fc[Cl]/BiOCl nanocomposite	10 min	10 mg	Ultrasonic conditions RT	EtOH/H <sub>2</sub> O	95	[137]
18	POM@Dy-PDA cations interspersed with POM anion	15 min	10 mol%	Reflux	H <sub>2</sub> O/EtOH	95	This work

Dy, dysprosium; MW, Microwave irradiation; PDA, 1,10-phenanthroline-2,9-dicarboxylic acid; POM, polyoxometalate; RT, Room Temperature.

between benzaldehyde and malononitrile with subsequent Michael addition of resorcinol with the Knoevenagel adduct (I). The final step involves an intramolecular cyclization (II) and tautomerization to give the desired 2-amino-4H-chromenes (III) (Scheme 2). It should be mentioned that in the POM catalyst, metal ions on the skeleton of POMs possess unoccupied orbital that can accept electron, thus acting as Lewis acid. Furthermore, lanthanoid coordination complexes have Lewis acid properties. They are hard Lewis acids in which hybridization using POMs improves catalytic efficacy. Therefore, in the POM@Dy-PDA catalyst, Mo atoms and Dy ions are active site in acid-catalyzed reaction.<sup>[65]</sup> The catalyst POM@Dy-PDA containing the acid sites enhances the electrophilicity of the carbonyl group of aromatic aldehydes which are subjected to dehydration to afford the Knoevenagel product and then aromatization.<sup>[122]</sup>

To show the merits of our novel catalyst, its catalytic activity was compared for the model system with that of several other potential catalysts (Table 9), such as potassium phthalimide-N-oxyl,<sup>[126]</sup> Mg/Al hydrotalcite,<sup>[112]</sup> tungstic acid functionalized mesoporous SBA-15,<sup>[127]</sup> nanozeolite clinoptilolite,<sup>[128]</sup> potassium phthalimide,<sup>[129]</sup> anhydrous sodium carbonate,<sup>[130]</sup> a triazine-based porous organic polymer (TPOP-2),<sup>[131]</sup> the ionic liquid 2-ethyl imidazolium acetate ([2-Eim]Oac),<sup>[110]</sup> Fe<sub>3</sub>O<sub>4</sub>-chitosan nanoparticles (Fe<sub>3</sub>O<sub>4</sub>-chitosan magnetic nanoparticles),<sup>[132]</sup> amino-appended  $\beta$ -cyclodextrins,<sup>[133]</sup> sulfonic acid-functionalized MIL-101(Cr) [MIL-101(Cr)-SO<sub>3</sub>H],<sup>[134]</sup> imidazolium ionic liquid functionalized magnetic multiwalled carbon nanotubes (CNTs-Fe<sub>3</sub>O<sub>4</sub>-IL),<sup>[135]</sup> highly monodisperse palladium nanoparticles supported with graphene oxide (Pd@GO),<sup>[136]</sup> palladium-ruthenium nanoparticles decorated on

graphene oxide (PdRu@GO),<sup>[111]</sup> and Fe<sub>3</sub>O<sub>4</sub>@SiO<sub>2</sub>-Benzim-Fc[Cl]/BiOCl nanocomposite.<sup>[137]</sup> The results show that our catalyst is superior in that it affords the desired products in better yield and shorter reaction times than many of the others. From the green chemistry point of view, the recyclability of the catalyst as well as employing H<sub>2</sub>O/EtOH as solvent renders this catalyst green and environmentally benign (Table 9).

### 3.4 | Reusability of the catalyst

A significant issue for heterogeneous catalysis is the easy separation of the catalyst and its recyclability. To investigate the catalyst reusability, the reaction of resorcinol, benzaldehyde, and malononitrile was performed in the presence of POM@Dy-PDA and the separated catalyst was reused in the same reaction for at least four times without observing any appreciable loss in its catalytic activity (for the first run 95% and for the fourth cycle 88% yields; Figure 11).

## 4 | CONCLUSIONS

We have synthesized and fully characterized a novel inorganic-organic hybrid POM@Dy-PDA by using a Keggin-type polyoxomolybdate (POM), the preorganized ligand PDA, and the dysprosium(III) ion with the formula 2[Dy<sub>4</sub>(PDA)<sub>4</sub>(H<sub>2</sub>O)<sub>11</sub>(SiMo<sub>12</sub>O<sub>40</sub>)]·7H<sub>2</sub>O. Its structure was unambiguously confirmed by single-crystal X-ray diffraction. It was successfully employed as an active heterogeneous catalyst in the efficient and green synthesis of aforementioned heterocyclic systems. We have also





investigated and described the role of strong anion- $\pi$  and hydrogen bonding interactions between the POM and the aromatic ring. These interactions play a crucial role in the 3D crystal packing formation. In addition, we compared the catalytic activity of the Keggin-type POM  $[\text{SiMo}_{12}\text{O}_{40}]^{4-}$  and our hybrid catalyst and the results show the effective combination of POM with metal coordination complexes, leading to the construction of efficient catalysts. The advantage of using the inorganic-organic hybrid than  $[\text{SiMo}_{12}\text{O}_{40}]^{4-}$  for catalyst reaction is increasing the specific surface area and number of active sites, decreasing the solubility, easy separation, short reaction, and excellent yields of the products. This combination of Ln(III) and Keggin-type POMs inaugurates a powerful class of porous catalysts for the different chemical transformations, which overcomes key limitations of previously established salts and Lewis acidic metals-based catalysts under low catalyst loading, the use of water scavengers, dry solvents, and additives for facilitating the specialized experimental setups commonly employed in the organic reactions. The merits recognized for this method are obtaining good to excellent yields, utilization of nontoxic solvents and catalyst, short reaction times, mild reaction conditions, wide functional group tolerance, and facile work-up procedure. Noticeably, this heterogeneous catalyst can be recovered effectively for four successive reaction cycles without significant loss of catalytic performance.

## ACKNOWLEDGEMENTS

M.M. gratefully acknowledges financial support from the Ferdowsi University of Mashhad (Grant No. 3/42203), the Iran Science Elites Federation (ISEF), Zeolite and Porous Materials Committee of Iranian Chemical Society and the Iran National Science Foundation (INSF). M.M. also acknowledges the Cambridge Crystallographic Data Centre (CCDC) for access to the Cambridge Structural Database. The authors also thankful Alzahra University and Iran Science Elites Federation for the given grant. JTM thanks Tulane University for support of the Tulane Crystallography Laboratory.

## ORCID

Masoud Mirzaei  <https://orcid.org/0000-0002-7256-4601>  
Majid M. Heravi  <https://orcid.org/0000-0003-2978-1157>

## REFERENCES

- [1] G. Brahmachari, B. Banerjee, *ACS Sustainable Chem. Eng.* **2013**, 2, 411.
- [2] A. Solhy, A. Elmakssoudi, R. Tahir, M. Karkouri, M. Larzek, M. Bousmina, M. Zahouily, *Green Chem.* **2010**, 12, 2261.
- [3] M. Boominathan, M. Nagaraj, S. Muthusubramanian, R. V. Krishnakumar, *Tetrahedron* **2011**, 67, 6057.
- [4] T. Raj, R. K. Bhatia, M. Sharma, A. K. Saxena, M. P. S. Ishar, *Eur. J. Med. Chem.* **2010**, 45, 790.
- [5] D.-O. Moon, K.-C. Kim, C.-Y. Jin, M.-H. Han, C. Park, K.-J. Lee, Y.-M. Park, Y. H. Choi, G.-Y. Kim, *Int. Immunopharmacol.* **2007**, 7, 222.
- [6] S. J. Mohr, M. A. Chirigos, F. S. Fuhrman, J. W. Pryor, *Cancer Res.* **1975**, 35, 3750.
- [7] M. Rueping, E. Sugiono, E. Merino, *Chem. – Eur. J.* **2008**, 14, 6329.
- [8] M. T. Flavin, J. D. Rizzo, A. Khilevich, A. Kucherenko, A. K. Sheinkman, V. Vilaychack, L. Lin, W. Chen, E. M. Greenwood, T. Pengsuparp, *J. Med. Chem.* **1996**, 39, 1303.
- [9] L. Bonsignore, G. Loy, D. Secci, A. Calignano, *Eur. J. Med. Chem.* **1993**, 28, 517.
- [10] A. Martínez-Grau, J. Marco, *Bioorg. Med. Chem. Lett.* **1997**, 7, 3165.
- [11] L. L. Andreani, E. Lapi, *Boll. Chim. Farm.* **1960**, 99, 583.
- [12] Y. L. Zhang, B. Z. Chen, K. Q. Zheng, M. L. Xu, X. H. Lei, Y. X. Bao, *In Chem. Abstr* **1982**17, 17, 96, 135383e.
- [13] N. Kishore, B. B. Mishra, V. Tripathi, V. K. Tiwari, *Fitoterapia* **2009**, 80, 149.
- [14] Y. Mehellou, E. De Clercq, *J. Med. Chem.* **2009**, 53, 521.
- [15] A. Matteelli, A. C. C. Carvalho, K. E. Dooley, A. Kritski, *Future Microbiol.* **2010**, 5, 849.
- [16] K. Schiemann, D. Finsinger, F. Zenke, C. Amendt, T. Knöchel, D. Bruge, H.-P. Buchstaller, U. Emde, W. Stähle, S. Anzali, *Bioorg. Med. Chem. Lett.* **2010**, 20, 1491.
- [17] K. Pradhan, S. Paul, A. R. Das, *Sci. Technol* **2014**, 4, 822.
- [18] R. Sarma, M. M. Sarmah, K. C. Lekhok, D. Prajapati, *Synlett* **2010**, 2010, 2847.
- [19] J. M. Khurana, S. Kumar, *Tetrahedron Lett.* **2009**, 50, 4125.
- [20] S. Abdolmohammadi, S. Balalaie, *Tetrahedron Lett.* **2007**, 48, 3299.
- [21] E. Esmaeilpour, J. Javidi, F. Dehghani, F. N. Dodeji, *RSC Adv.* **2015**, 5, 26625.
- [22] K. S. Pandit, P. V. Chavan, U. V. Desai, M. A. Kulkarni, P. P. Wadgaonkar, *New J. Chem.* **2015**, 39, 4452.
- [23] R. Ballini, G. Bosica, M. L. Conforti, R. Maggi, A. Mazzacani, P. Righi, G. Sartori, *Tetrahedron* **2001**, 57, 1395.
- [24] Y.-F. Han, M. Xia, *Curr. Org. Chem.* **2010**, 14, 379.
- [25] A. Q. Zhang, M. Zhang, H. H. Chen, J. Chen, H. Y. Chen, *Synth. Commun.* **2007**, 37, 231.
- [26] B. S. Kumar, N. Srinivasulu, R. H. Udipi, B. Rajitha, Y. T. Reddy, P. N. Reddy, P. S. Kumar, *J. Heterocyclic Chem.* **2006**, 43, 1691.
- [27] O. Rosati, M. Curini, M. C. Marcotullio, G. Oball-Mond, C. Pelucchini, A. Procopio, *Synthesis* **2010**, 2010, 239.
- [28] Y.-M. Ren, C. Cai, *Cat. Com.* **2008**, 9, 1017.
- [29] N. V. Lakshmi, S. E. Kiruthika, P. T. Perumal, *Synlett* **2011**, 2011, 1389.
- [30] R. M. N. Kalla, S. J. Byeon, M. S. Heo, I. Kim, *Tetrahedron* **2013**, 69, 10544.
- [31] A. Shaabani, R. Ghadari, S. Ghasemi, M. Pedarpour, A. H. Rezayan, A. Sarvary, S. W. Ng, *J. Comb. Chem.* **2009**, 11, 956.

- [32] T. S. Jin, J. C. Xiao, S. J. Wang, T. S. Li, X. R. Song, *Synlett* **2003**, 2003, 2001.
- [33] M. M. Heravi, K. Bakhtiari, V. Zadsirjan, F. F. Bamoharram, O. M. Heravi, *Bioorg. Med. Chem. Lett.* **2007**, 17, 4262.
- [34] D. Kumar, V. B. Reddy, B. G. Mishra, R. K. Rana, M. N. Nadagouda, R. S. Varma, *Tetrahedron* **2007**, 63, 3097.
- [35] L. Chen, Y. Q. Li, X. J. Huang, W. J. Zheng, *Heteroatom Chem.* **2009**, 20, 91.
- [36] G. Centi, S. Perathoner, *Catal. Today* **2003**, 77, 287.
- [37] Q. W. Song, Z. H. Zhou, L. N. He, *Green Chem.* **2017**, 19, 3707.
- [38] M. Alipour, O. Akintola, A. Buchholz, M. Mirzaei, H. Eshtiagh-Hosseini, H. Görls, W. Plass, *Eur. J. Inorg. Chem.* **2016**, 2016, 5356.
- [39] M. M. Heravi, M. Mirzaei, S. Y. S. Beheshtiha, V. Zadsirjan, F. Mashayekh Ameli, M. Bazargan, *Appl. Organomet. Chem.* **2018**, 32, e4479.
- [40] M. Arefian, M. Mirzaei, H. Eshtiagh-Hosseini, *J. Mol. Struct.* **2018**, 1156, 550.
- [41] G. J. Cao, J. D. Liu, T. T. Zhuang, X. H. Cai, S. T. Zheng, *Chem. Commun.* **2012**, 51, 2048.
- [42] A. Lesbani, R. Kawamoto, S. Uchida, N. Mizuno, *Inorg. Chem.* **2008**, 47, 3349.
- [43] R. Neumann, M. Levin, *J. Am. Chem. Soc.* **1992**, 114, 7278.
- [44] L. Manfred, J. Helmut, *Tetrahedron Lett.* **1992**, 33, 1795.
- [45] S. L. Linguito, X. Zhang, M. Padmanabhan, A. V. Biradar, T. Xu, T. J. Emge, T. Asefa, J. Li, *New J. Chem.* **2013**, 37, 2894.
- [46] H. Wang, Y. P. Chen, Z. C. You, M. X. Zhou, N. Zhang, Y. Q. Sun, *Chin. Chem. Lett.* **2015**, 26, 187.
- [47] J. Macht, M. J. Janik, M. Neurock, E. Iglesia, *Angew. Chem. Int. Ed.* **2007**, 46, 7868.
- [48] K. Amani, F. Maleki, *J. Iran. Chem. Soc.* **2007**, 4, 238.
- [49] S. Hayashi, S. Yamazoe, K. Koyasu, T. Tsukuda, *RSC Adv.* **2016**, 6, 16239.
- [50] K. Kamata, K. Sugahara, *Catalysts* **2017**, 7, 345.
- [51] Z. Long, Y. Zhou, G. Chen, W. Ge, J. Wang, *Sci. Rep.* **2014**, 4, 3651.
- [52] N. Mizuno, K. Yamaguchi, K. Kamata, *Coord. Chem. Rev.* **2005**, 249, 1944.
- [53] N. Mizuno, M. Misono, *Chem. Rev.* **1998**, 98, 199.
- [54] T. A. Duarte, A. C. Estrada, M. M. Simões, I. C. Santos, A. M. Cavaleiro, M. G. P. Neves, J. A. Cavaleiro, *Catal. Sci. Technol.* **2015**, 5, 351.
- [55] L. S. Nogueira, S. Ribeiro, C. M. Granadeiro, E. Pereira, G. Feio, L. Cunha-Silva, S. S. Balula, *Dalton Trans.* **2014**, 43, 9518.
- [56] E. Poli, R. De Sousa, F. Jerome, Y. Pouilloux, J. M. Clacens, *Catal. Sci. Technol.* **2012**, 2, 910.
- [57] K. Yamaguchi, C. Yoshida, S. Uchida, N. Mizuno, *J. Am. Chem. Soc.* **2005**, 127, 530.
- [58] Y. Zhou, G. Chen, Z. Long, J. Wang, *RSC Adv.* **2014**, 4, 42092.
- [59] X. Cai, Q. Wang, Y. Liu, J. Xie, Z. Long, Y. Zhou, J. Wang, *Sustain. Chem. Eng.* **2016**, 4, 4986.
- [60] Y. Leng, J. Liu, P. Jiang, J. Wang, *ACS Sustainable Chem. Eng.* **2014**, 3, 170.
- [61] A. Dolbecq, E. Dumas, C. R. Mayer, P. Mialane, *Chem. Rev.* **2010**, 110, 6009.
- [62] N. Lotfian, M. M. Heravi, M. Mirzaei, M. Daraie, *J. Mol. Struct.* **2020**, 1199, 126953.
- [63] M. Daraie, M. M. Heravi, M. Mirzaei, N. Lotfian, *Appl. Organomet. Chem.* **2019**, 33, e5058.
- [64] M. A. Fashapoyeh, M. Mirzaei, H. Eshtiagh-Hosseini, A. Rajagopal, M. Lechner, R. Liu, C. Streb, *Chem. Commun.* **2018**, 54, 10427.
- [65] N. Lotfian, M. M. Heravi, M. Mirzaei, B. Heidari, *Appl. Organomet. Chem.* **2019**, 33, e4808.
- [66] X. Chen, Z. Wang, R. Zhang, L. Xu, D. Sun, *Chem. Commun.* **2017**, 53, 10560.
- [67] T. P. Hu, Y. Q. Zhao, Z. Jagličić, K. Yu, X. P. Wang, D. Sun, *Inorg. Chem.* **2015**, 54, 7415.
- [68] Y. W. Li, L. Y. Guo, H. F. Su, M. Jagodič, M. Luo, X. Q. Zhou, S. Y. Zeng, C. H. Tung, D. Sun, L. S. Zheng, *Inorg. Chem.* **2017**, 56, 2481.
- [69] V. Mirkhani, M. Moghadam, S. Tangestaninejad, I. Mohammadpoor-Baltork, N. Rasouli, *Cat. Com.* **2008**, 9, 2171.
- [70] V. Mirkhani, M. Moghadam, S. Tangestaninejad, I. Mohammadpoor-Baltork, N. Rasouli, *Cat. Com.* **2008**, 9, 219.
- [71] M. M. Heravi, G. Rajabzadeh, F. F. Bamoharram, N. Seifi, *J. Mol. Catal. A: Chem.* **2006**, 256, 238.
- [72] M. M. Heravi, R. Motamedi, N. Seifi, F. F. Bamoharram, *J. Mol. Catal. A: Chem.* **2006**, 249, 1.
- [73] S. Taleghani, M. Mirzaei, H. Eshtiagh-Hosseini, A. Frontera, *Coord. Chem. Rev.* **2016**, 309, 84.
- [74] A. Najafi, M. Mirzaei, J. T. Mague, *CrystEngComm* **2016**, 18, 6724.
- [75] M. Mirzaei, H. Eshtiagh-Hosseini, A. Hassanpoor, *Inorg. Chim. Acta* **2019**, 484, 332.
- [76] M. Samaniyan, M. Mirzaei, R. Khajavian, H. Eshtiagh-Hosseini, C. Streb, *ACS Catal.* **2019**, 9, 10174.
- [77] M. Mirzaei, H. Eshtiagh-Hosseini, M. Alipour, A. Bauzá, J. T. Mague, M. Korabik, A. Frontera, *Dalton Trans.* **2015**, 44, 8824.
- [78] S. Derakhshanrad, M. Mirzaei, A. Najafi, C. Ritchie, A. Bauzá, A. Frontera, J. T. Mague, *Acta Crystallogr., Sect. C: Struct. Chem.* **2018**, 74, 1300.
- [79] A. Amiri, M. Mirzaei, S. Derakhshanrad, *Microchim. Acta* **2019**, 186, 534.
- [80] M. M. Heravi, S. Sadjadi, *J. Iran. Chem. Soc.* **2009**, 6, 1.
- [81] M. M. Heravi, Z. Faghihi, *J. Iran. Chem. Soc.* **2014**, 11, 209.
- [82] M. M. Heravi, M. Vazin Fard, Z. Faghihi, *Green Chem. Lett.* **2013**, 6, 282.
- [83] M. Lissel, H. J. in de Wal, R. Neumann, *Tetrahedron Lett.* **1992**, 33, 1795.
- [84] M. Mirzaei, H. Eshtiagh-Hosseini, M. Alipour, A. Frontera, *Coord. Chem. Rev.* **2014**, 275, 1.
- [85] M. Wei, C. He, Q. Sun, Q. Meng, C. Duan, *Inorg. Chem.* **2007**, 46, 5957.
- [86] H. An, Z. Han, T. Xu, *Inorg. Chem.* **2010**, 49, 11403.
- [87] W.-F. Zhao, C. Zou, L.-X. Shi, J.-C. Yu, G.-D. Qian, C.-D. Wu, *Dalton Trans.* **2012**, 41, 10091.
- [88] X. Feng, L. Liu, L. Y. Wang, H. L. Song, Z. Q. Shi, X. H. Wu, S. W. Ng, *J. Solid State Chem.* **2013**, 206, 277.

- [89] P. Comba, W. Schiek, *Coord. Chem. Rev.* **2003**, 238, 21.
- [90] R. D. Hancock, A. E. Martell, *Chem. Rev.* **1989**, 89, 1875.
- [91] R. D. Hancock, D. L. Melton, J. M. Harrington, F. C. McDonald, R. T. Gephart, L. L. Boone, S. B. Jones, N. E. Dean, J. R. Whitehead, G. M. Cockrell, *Coord. Chem. Rev.* **2007**, 251, 1678.
- [92] D. L. Melton, D. G. VanDerveer, R. D. Hancock, *Inorg. Chem.* **2006**, 45, 9306.
- [93] N. E. Dean, R. D. Hancock, C. L. Cahill, M. Frisch, *Inorg. Chem.* **2008**, 47, 2000.
- [94] M. D. Ogden, S. I. Sinkov, M. Nilson, G. J. Lumetta, R. D. Hancock, K. L. Nash, *J. Solution, Chem* **2013**, 42, 211.
- [95] M. M. Heravi, S. Khaghaninejad, M. Mostofi, *Adv. Heterocycl. Chem.* **2014**, 112, 1.
- [96] M. M. Heravi, B. Talaei, *Adv. Heterocycl. Chem.* **2015**, 114, 147.
- [97] M. M. Heravi, V. F. Vavsari, *Adv. Heterocycl. Chem.* **2015**, 114, 77.
- [98] M. M. Heravi, B. Talaei, *Adv. Heterocycl. Chem.* **2016**, 118, 195.
- [99] M. M. Heravi, L. Ranjbar, F. Derikvand, B. Alimadadi, H. A. Oskooie, F. F. Bamoharram, *Mol. Diversity* **2008**, 12, 181.
- [100] S. Sadjadi, M. M. Heravi, M. Malmir, *Appl. Organomet. Chem.* **2018**, 32, e4029.
- [101] R. Mirsafaei, M. M. Heravi, T. Hosseinnejad, S. Ahmadi, *Appl. Organomet. Chem.* **2016**, 30, 823.
- [102] M. M. Heravi, F. Mousavizadeh, N. Ghobadi, M. Tajbakhsh, *Tetrahedron Lett.* **2014**, 55, 1226.
- [103] R. Mirsafaei, M. M. Heravi, S. Ahmadi, M. H. Moslemin, T. Hosseinnejad, *J. Mol. Catal. A: Chem.* **2015**, 402, 100.
- [104] C. J. Chandler, L. W. Deady, J. A. Reiss, *J. Heterocyclic Chem.* **1981**, 18, 599.
- [105] R. Thouvenot, M. Fournier, R. Franck, C. Rocchiccioli-Deltcheff, *Inorg. Chem.* **1984**, 23, 598.
- [106] J. Coates, *Encyclopedia of analytical chemistry: applications, theory and instrumentation* **2006**.
- [107] K. Barteau, J. Lyons, I. Song, M. Barteau, *Top. Catal.* **2006**, 41, 55.
- [108] R. S. Yelamanchili, A. Walther, A. H. Müller, J. Breu, *Chem. Commun.* **2008**, 4, 489.
- [109] H. T. Evans Jr., M. T. Popev, *Inorg. Chem.* **1984**, 23, 501.
- [110] M. Ghorbani, S. Noura, M. Oftadeh, M. A. Zolfigol, M. H. Soleimani, K. Behbodi, *J. Mol. Liq.* **2015**, 212, 291.
- [111] B. Şen, N. Lolak, Ö. Paralı, M. Koca, A. Şavk, S. Akocak, F. Şen, *Nano-Struct. Nano-Objects* **2017**, 12, 33.
- [112] S. R. Kale, S. S. Kahandal, A. S. Burange, M. B. Gawande, R. V. Jayaram, *Catal. Sci. Technol.* **2013**, 3, 2050.
- [113] H. Mehrabi, H. Abusaidi, *J. Iran. Chem. Soc.* **2010**, 7, 890.
- [114] J. M. Khurana, B. Nand, P. Saluja, *Tetrahedron* **2010**, 66, 5637.
- [115] S. Khodabakhshi, F. Marahel, A. Rashidi, M. K. Abbasabadi, *J. Chin. Chem. Soc.* **2015**, 62, 389.
- [116] R. Teimuri-Mofrad, S. Esmati, S. Tahmasebi, M. Gholamhosseini-Nazari, *J. Org. Chem.* **2018**, 870, 38.
- [117] M. Khoobi, L. Ma'mani, F. Rezazadeh, Z. Zareie, A. Foroumadi, A. Ramazani, A. Shafiee, *J. Mol. Catal-a: Chem.* **2012**, 359, 74.
- [118] V. A. Vasin, S. G. Kostryukov, I. Bolusheva, V. V. Razin, *Russ. J. Org. Chem.* **1993**, 29, 1118.
- [119] S. Tu, H. Jiang, F. Fang, Y. Feng, S. Zhu, T. Li, X. Zhang, D. Shi, *J. Chem. Res.* **2004**, 2004, 396.
- [120] H. Mecadon, M. R. Rohman, M. Rajbangshi, B. Myrboh, *Tetrahedron Lett.* **2011**, 52, 2523.
- [121] Y. A. Tayade, S. A. Padvi, Y. B. Wagh, D. S. Dalal, *Tetrahedron Lett.* **2015**, 56, 2441.
- [122] S. Khaksar, A. Rouhollahpour, S. M. Talesh, *J. Fluorine Chem.* **2012**, 141, 11.
- [123] M. G. Dekamin, M. Eslami, A. Maleki, *Tetrahedron* **2013**, 69, 1074. bM. Saha, A. K. Pal, *Synth. Commun.* **2013**, 43, 1708.
- [124] S. K. Kundu, J. Mondal, A. Bhaumik, *Dalton Trans.* **2013**, 42, 10515.
- [125] S. M. Baghbanian, N. Rezaei, H. Tashakkorian, *Green Chem.* **2013**, 15, 3446.
- [126] M. G. Dekamin, M. Eslami, *Green Chem.* **2014**, 16, 4914.
- [127] O. H. Qareaghaj, S. Mashkouri, M. R. Naimi-Jamal, G. Kaupp, *RSC Adv.* **2014**, 4, 48191.
- [128] S. K. Kundu, A. Bhaumik, *RSC Adv.* **2015**, 5, 32730.
- [129] J. Safari, L. Javadian, *Ultrason. Sonochem.* **2015**, 22, 341.
- [130] Y. Ren, B. Yang, X. Liao, *Catal. Sci. Technol.* **2016**, 6, 4283.
- [131] M. Saikia, L. Saikia, *RSC Adv.* **2016**, 6, 15846.
- [132] Z. Zarnegar, J. Safari, *New J. Chem.* **2016**, 40, 7986.
- [133] S. Akocak, B. Şen, N. Lolak, A. Şavk, M. Koca, S. Kuzu, F. Şen, *Nano-Struct. Nano-Objects* **2017**, 11, 25.
- [134] J. Safari, M. Heydarian, Z. Zarnegar, *Arab. J. Chem.* **2017**, 10, S2994.
- [135] R. Mohammadi, S. Esmati, M. Gholamhosseini-Nazari, R. Teimuri-Mofrad, *New J. Chem.* **2019**, 43, 135.
- [136] Y. Wang, C. Yue, X. Li, J. Luo, *C. R. Chim.* **2016**, 19, 1021.
- [137] S. Shinde, S. Damate, S. Morbale, M. Patil, S. S. Patil, *RSC Adv.* **2017**, 7, 7315.
- [138] R. Teimuri-Mofrad, M. Gholamhosseini-Nazari, E. Payami, S. Esmati, *Appl. Organomet. Chem.* **2018**, 32, e3955.
- [139] J. Albadi, A. Mansourneshad, M. Darvishi-Paduk, *Chin. Chem. Lett.* **2013**, 24, 208.
- [140] O.V. Dolomanov, L.J. Bourhis, R.J. Gildea, J.A. Howard, H. Puschmann, *J. Appl. Cryst.* **2009**, 42, 339.
- [141] G.M. Sheldrick, *Acta Cryst. A.* **2015**, 71, 3.

## SUPPORTING INFORMATION

Additional supporting information may be found online in the Supporting Information section at the end of this article.

**How to cite this article:** Hosseinzadeh-Baghan S, Mirzaei M, Eshtiagh-Hosseini H, Zadsirjan V, Heravi MM, Mague JT. An inorganic–organic hybrid material based on a Keggin-type polyoxometalate@Dysprosium as an effective and green catalyst in the synthesis of 2-amino-4H-chromenes via multicomponent reactions. *Appl Organomet Chem.* 2020;e5793. <https://doi.org/10.1002/aoc.5793>